Available online at www.sciencedirect.com

SCIENCE DIRECT

Virology 328 (2004) 282–291

VIROLOGY

www.elsevier.com/locate/yviro

Role for a region of helically unstable DNA within the Epstein–Barr virus latent cycle origin of DNA replication *oriP* in origin function

Zhanna Polonskaya[a,1], Craig J. Benham[b], Janet Hearing[a,*]

[a]*Department of Molecular Genetics and Microbiology, Stony Brook University, Stony Brook, NY 11794, USA*
[b]*Department of Mathematics, University of California at Davis, Davis, CA 95616, USA*

Received 7 May 2004; returned to author for revision 27 May 2004; accepted 23 July 2004
Available online 2 September 2004

Abstract

The minimal replicator of the Epstein–Barr virus (EBV) latent cycle origin of DNA replication *oriP* is composed of two binding sites for the Epstein–Barr virus nuclear antigen-1 (EBNA-1) and flanking inverted repeats that bind the telomere repeat binding factor TRF2. Although not required for minimal replicator activity, additional binding sites for EBNA-1 and TRF2 and one or more auxiliary elements located to the right of the EBNA-1/TRF2 sites are required for the efficient replication of *oriP* plasmids. Another region of *oriP* that is predicted to be destabilized by DNA supercoiling is shown here to be an important functional component of *oriP*. The ability of DNA fragments of unrelated sequence and possessing supercoiled-induced DNA duplex destabilized (SIDD) structures, but not fragments characterized by helically stable DNA, to substitute for this component of *oriP* demonstrates a role for the SIDD region in the initiation of *oriP*-plasmid DNA replication.

Keywords: Epstein–Barr virus; *oriP*; DNA unwinding element; EBNA-1; SIDD structures

Introduction

The Epstein–Barr virus (EBV) genome is usually maintained as a single- or multiple-copy plasmid in latently infected cells (Mecsas and Sugden, 1987; Yates, 1996). EBV latent cycle DNA replication may initiate at one of several sites and each plasmid is replicated once per cell division cycle during S phase (Adams, 1987; Little and Schildkraut, 1995; Mecsas and Sugden, 1987; Norio and Schildkraut, 2001; Yates, 1996). The best-characterized EBV latent cycle replication origin is called *oriP* (Yates et al., 1984). Although this origin is not required for the establishment of the EBV genome as a replicating, extrachromosomal plasmid upon infection of EBV-negative Burkitt's lymphoma cells (Norio et al., 2000), the presence of *oriP* within all EBV isolates and the high conservation of its sequence suggests an essential role for this origin in the establishment of EBV latency following the infection of quiescent B lymphocytes in vivo (Koons et al., 2001). A 2.2-kb fragment of EBV DNA encompassing *oriP* provides cell cycle-regulated replication and stable maintenance of plasmids bearing this fragment (Yates and Guan, 1991) and contains several distinct functional elements (Fig. 1). An element composed of 20 tandemly arrayed binding sites for the EBV nuclear antigen-1 (EBNA-1) designated FR (Family of Repeats) is present at the left end of *oriP*. FR is required for the maintenance of the EBV genome and plasmids bearing *oriP* in dividing cells (Harrison et al., 1994; Reisman et al., 1985; Yates et al., 1984) but is dispensable for the initiation of replication within *oriP* (Harrison et al., 1994; Shirakata and Hirai, 1998; Yates et al., 2000). The replicator of *oriP* is located approximately 1-kb from FR and is coincident with, or positioned near,

* Corresponding author. Department of Molecular Genetics and Microbiology, Stony Brook University, Life Sciences 130, Stony Brook, NY 11794. Fax: +1 631 632 9797.
E-mail address: jhearing@ms.cc.sunysb.edu (J. Hearing).
[1] Current address: Department of Cell Biology, Albert Einstein College of Medicine, New York, NY 10461, USA.

0042-6822/$ - see front matter © 2004 Elsevier Inc. All rights reserved.
doi:10.1016/j.virol.2004.07.023

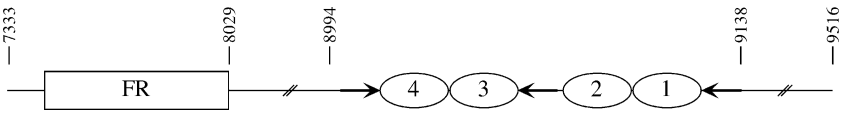

Fig. 1. EBV sequence present within pHEBo-1 and pHEBo-1.1. The nucleotide coordinates for the fragment of EBV DNA (B95-8 isolate) encompassing *oriP* and present within the parental plasmids used in this study, pHEBo-1 and pHEBo-1.1, are shown above a schematic of *oriP* (not drawn to scale). The positions of FR, the four EBNA-1 binding sites within the replicator (numbered ovals), and TRF2 binding sites (arrows flanking the EBNA-1 sites) are indicated.

the origin of DNA replication (Gahn and Schildkraut, 1989). The replicator contains four binding sites for EBNA-1, all of which are required for maximal replicator activity (Koons et al., 2001; Yates et al., 2000), and three 9-bp repeats flanking the EBNA-1 sites that are binding sites for the telomere repeat binding factors 1 and 2 (TRF2) (Deng et al., 2002). One or more undefined elements that are not absolutely required for replicator function but increase the efficiency with which replication initiates are located to the right of the EBNA-1 and TRF2 binding sites (Koons et al., 2001).

The binding of EBNA-1 to sites within the replicator bends the DNA at the center of binding but EBNA-1, by itself, is unable to unwind the DNA (Bashaw and Yates, 2001; Frappier and O'Donnell, 1992; Hearing et al., 1992). This information, together with the observations that EBNA-1 is the sole viral protein required for the replication of plasmids bearing *oriP* (Yates et al., 1985) and that *oriP* plasmid replication occurs once per cell cycle in synchrony with the duplication of the cellular chromosomes (Adams, 1987; Shirakata et al., 1999), supported the hypothesis that EBNA-1 recruits proteins to the *oriP* replicator that are involved in the initiation of cellular DNA replication. This prediction was fulfilled in part by the demonstration of the binding of the human origin recognition complex (ORC) and the replication licensing MCM proteins to the replicator of *oriP* in vivo (Chaudhuri et al., 2001; Schepers et al., 2001). The recruitment of ORC and MCM subunits to *oriP* was eliminated by deletion of the four EBNA-1 binding sites, the three TRF2 binding sites, and 24 bp of left-hand flanking sequence within the replicator (deletion of EBV nt 8994–9134; (Fig. 1) (Chaudhuri et al., 2001) but the molecular interactions that allow ORC and MCM proteins to associate functionally with the *oriP* replicator are not known.

In addition to the presence of one or more binding sites for an origin recognition protein that recruits other replication proteins to the origin, the well-characterized origins of the papovavirus SV40 and *Saccharomyces cerevisiae*, as well as *oriC* of *Escherichia coli*, contain elements at, or adjacent to, the origin that facilitate origin unwinding (Kowalski and Eddy, 1989; Lin and Kowalski, 1997; Natale et al., 1992). These DNA unwinding elements (DUEs) are characterized by intrinsic helical instability that may be predicted by a computer program that utilizes the thermodynamic properties of nearest-neighbor dinucleotides (Natale et al., 1992). Some, but not all, DUEs contain sites of hypersensitivity to single-strand specific nucleases in vitro in the absence of the origin recognition protein (Borowiec and Hurwitz, 1988; Kowalski and Eddy, 1989; Lin and Kowalski, 1994; Umek and Kowalski, 1988). These DUEs may be functionally replaced by unrelated sequences that exhibit helical instability (Kowalski and Eddy, 1989; Umek and Kowalski, 1988). We have examined *oriP* for the presence of potential DUEs using a statistical mechanical method (Benham, 1993) and have identified a supercoiled-induced DNA duplex destabilized (SIDD) structure within *oriP*. Deletion of this SIDD element greatly reduced the efficiency with which replication initiated within *oriP*. The replication defect of a plasmid lacking this element was completely rescued by unrelated DNA sequences harboring helically unstable DNA but not by unrelated DNA sequences characterized by high helical stability. These results demonstrate a functional role for a SIDD structure in the initiation of DNA replication within *oriP*.

Results and discussion

Previous analysis of the helical stability of an *oriP*-bearing plasmid using the thermodynamic properties of nearest-neighbor dinucleotides identified *oriP* FR as the least helically stable region within *oriP* (Williams and Kowalski, 1993) and, in the absence of EBNA-1, the single-strand-specific nucleases P1 and T7 cleaved *oriP*-bearing plasmids within FR (Orlowski and Miller, 1991; Williams and Kowalski, 1993). However, EBNA-1 is bound to the 20 sites within FR throughout the cell cycle and non-base-paired nucleotides have not been detected within FR in vivo or in vitro (Frappier and O'Donnell, 1992; Hearing et al., 1992; Hsieh et al., 1993). To identify potential DUEs within *oriP* that may not have been identified in previous studies, we analyzed *oriP* both in the context of the EBV genome and a small recombinant *oriP*-plasmid (pHEBo-1.1) for the presence of SIDD structures using a statistical mechanical method that measures intrinsic local instability as well as global competition among all sites within a stressed domain and identifies regions within superhelical DNA molecules that are destabilized as well as denatured (Benham, 1992, 1993). The results of this analysis are presented as a destabilization profile in which the incremental free energy $G(x)$ necessary to guarantee denaturation of the base pair at position x is plotted versus sequence location (Fig. 2). High values of $G(x)$ indicate that the bp position is not destabilized by superhelical stresses and, conversely, low values of $G(x)$ identify positions where a base pair is significantly destabilized. The most highly destabilized

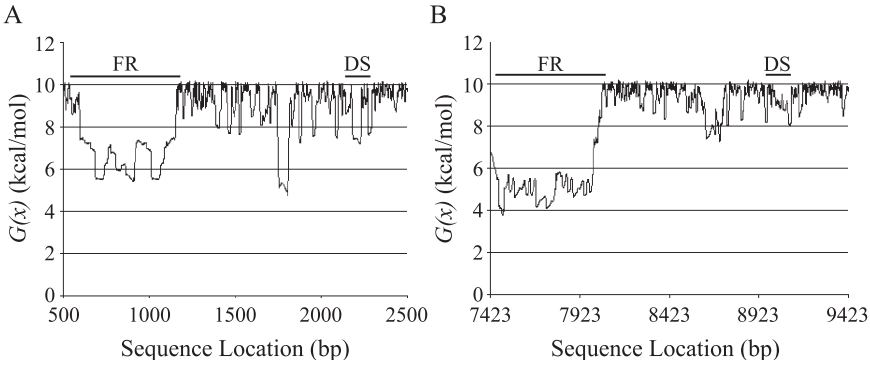

Fig. 2. Helix destabilization profiles for *oriP*. The destabilization profiles show the incremental free energy $G(x)$ required to denature the base pair at position x for *oriP* within pHEBo-1.1 (panel A) and the EBV genome (panel B). The positions of FR and the dyad symmetry element (DS) containing the replicator are indicated by bars over the top of each profile.

region within pHEBo-1.1 is an A + T-rich region within the 3′ region of the β-lactamase gene (around bp position 5800) that has been previously characterized as a site of stable DNA unwinding in supercoiled pBR322 DNA (Kowalski et al., 1988) and the second most highly destabilized region (around bp position 6700) is within the promoter region of the β-lactamase gene (not shown). This latter destabilized region was also shown to be sensitive to a single-strand-specific nuclease in a pBR322 derivative lacking the destabilized region within the 3′ region of the β-lactamase gene (Kowalski et al., 1988). The locations of these regions are consistent with previous findings that sites within duplex DNA predicted to be destabilized by superhelical stresses are associated with *cis* regulatory loci including gene promoters and terminators (Benham, 1992, 1993). The helix destabilization profile also predicts that a sequence at approximately bp position 1790 (centered at EBV bp position 8660; Fig. 2A) between FR and the replicator is likely to be destabilized by superhelical stresses. This region, as well as *oriP* FR, is also predicted to be helically unstable in the context of the EBV genome (Fig. 2B). Neither of these regions within *oriP*, regardless of sequence context, are predicted to be unwound at a physiological superhelical density of −0.055. Differences in $G(x)$ for the same region of *oriP* when in the context of the EBV genome and in pHEBo-1.1 are due to the competition that exists between sites within a single superhelical domain (Benham, 1996).

Early genetic analyses of *oriP* relied upon the determination of *oriP* plasmid copy number in stable transformants of EBNA-1-expressing cells as a measure of replication efficiency and concluded that the sequence between FR and the replicator is not absolutely required for replicator activity (Fig. 1) (Reisman et al., 1985). We have found that the measurement of plasmid copy number is not a reliable method for the identification of elements that are not essential for replication to initiate from within *oriP* but are required for replication to occur with 100% efficiency (i.e., once per cell cycle) (Koons et al., 2001). We therefore analyzed the impact of deletions within *oriP* upon replication efficiency using a quantitative short-term replication assay to determine if the sequence encompassing the SIDD structure predicted between FR and the EBNA-1/TRF2 binding sites is required for efficient plasmid replication. Test plasmids were co-electroporated into an EBV-positive Burkitt's lymphoma cell line (Raji) with a plasmid harboring intact *oriP* and the relative amount of replicated test and control plasmid DNA present within the cells after three cell generations was measured by Southern blotting (Koons et al., 2001). The replication efficiency of an *oriP* plasmid lacking 642 bp between FR and the EBNA-1/TRF2 binding sites (pHEBo-1.1-Δ8353–8994; Fig. 1) was compared to the replication efficiency of the parental plasmid containing intact *oriP* (pHEBo-1.1). The positions of relevant restriction enzyme sites within the plasmids used in this study and a representative Southern blot showing the results of this experiment are shown in Figs. 3 and 4, respectively, and the replication efficiencies of the plasmids examined in this experiment are presented in Table 1. Deletion of EBV nt 8353–8994 from pHEBo-1.1 reduced replication efficiency to approximately 30% per cell cycle. The magnitude of the effect of deleting these nucleotides was greater than the effect of deleting an auxiliary element(s) present within EBV nt 9138–9516 from pHEBo-1.1 (Table 1; $P < 0.01$). Deletion of both nt 8353–8994 and 9138–9516 from pHEBo-1.1 reduced replication efficiency to a level that was indistinguishable from that of a pHEBo-1.1-derivative lacking essential elements of the replicator (pHEBo-2.2; $P = 0.33$) (Koons et al., 2001).

To address the possibility that helically unstable DNA within EBV nt 8353–8994 contributes to *oriP* replicator function and its absence is responsible for the replication defect of pHEBo-1.1Δ8353–8994 (Fig. 4 and Table 1), we replaced these nucleotides within pHEBo-1.1 with four fragments of EBV DNA of about the same size. Two of these substitutions were created with DNA fragments of predicted low helical instability (sub1 and sub2; 672 and 650 bp, respectively) and two were constructed with fragments of predicted moderate to high helical instability (sub3 and sub4;

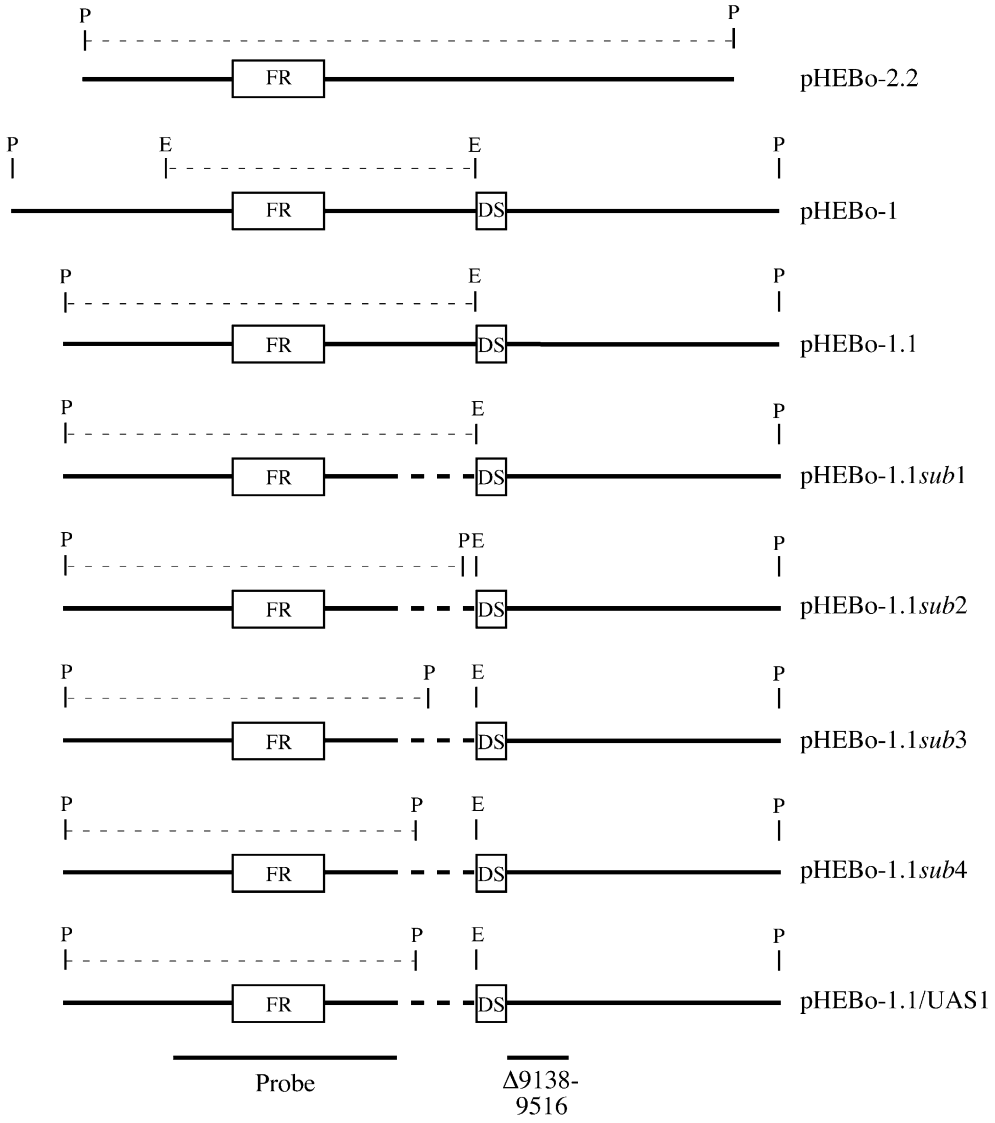

Fig. 3. pHEBo-1 and its derivatives. The locations of FR, DS, and sites cleaved by restriction enzymes used in replication assays are shown (P, *Pst*1; E, *Eco*RV). Sequences substituted for EBV nt 8353–8994 within pHEBo-1.1*sub*1, pHEBo-1.1*sub*2, pHEBo-1.1*sub*3, pHEBo-1.1*sub*4, and pHEBo-1.1/UAS1 are indicated by the heavy dashed line. The region of pHEBo-1 used as probe in replication assays is shown at the bottom of the figure and the restriction enzyme fragments that hybridized to the probe in the Southern blots shown in Figs. 4 and 6 are indicated by the light dashed line above each plasmid.

640 and 654 bp, respectively). None of these fragments originated from a region of EBV DNA that contains multiple latent cycle replication initiation sites (Little and Schildkraut, 1995; Norio and Schildkraut, 2001). The destabilization profiles for these DNA fragments within *oriP* of pHEBo-1.1 are shown in Fig. 5 and the profiles for the sub1 and sub2 DNAs in the context of pHEBo-1.1 and the EBV genome closely resembled one another (Fig. 5 and data not shown). Both sub3 and sub4 were predicted to be more helically unstable when present within the EBV genome (Fig. 5). Plasmids containing sequences with predicted moderate to high helical instability in place of EBV nt 8353–8994 were replicated as efficiently as pHEBo-1.1 (pHEBo-1.1*sub*3 and pHEBo-1.1*sub*4; Fig. 6 and Table 2). In contrast, plasmids containing sequences with predicted low helical instability in place of EBV nt 8353–8994 exhibited replication defects (compare pHEBo-1.1*sub*1 and pHEBo-1.1*sub*2 to pHEBo-1.1; $P < 0.01$ for both comparisons). Similarly, substitution of fragments of predicted high helical instability (sub3 and sub4) for EBV nt 8353–8994 increased the replication efficiency of pHEBo-1.1Δ8353–8994;9138–9516 to approximately 80–90%, while insertion of fragments of predicted low helical instability (sub1 and sub2) only increased the replication efficiency of pHEBo-1.1Δ8353–8994;9138–9516 to 30–35% (Fig. 6 and Table 2).

We also replaced the *oriP* SIDD element centered at EBV nt 8660 with a DNA fragment from the *E. coli* genome that contains the upstream activating sequence (UAS1) from the *ilv*P_G promoter (Fig. 7) to determine if the well-characterized SIDD element in the *ilv*P_G UAS1 could substitute functionally for the *oriP* SIDD element (Sheridan et al., 1998; Sheridan et al., 1999). The *ilv*P_G UAS1 was

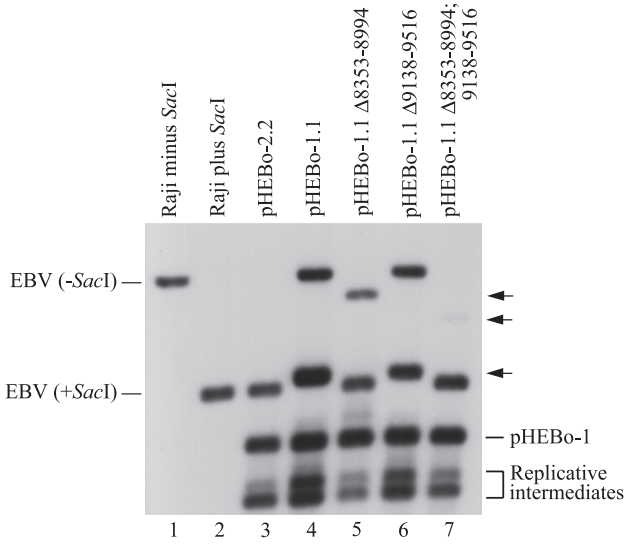

Fig. 4. Deletion of sequences flanking the EBNA-1/TRF2 sites reduces replication efficiency. EBV-positive Burkitt's lymphoma cells (Raji) were co-electroporated with pHEBo-1 and the test plasmids indicated above each lane and *Dpn1*-resistant, low molecular weight DNA were isolated 72 h later. Each sample was also digested with restriction enzymes that produce fragments of differing size from the internal control plasmid pHEBo-1 and the test plasmid (*Eco*RV and *Pst*1), and analyzed by Southern blotting. The experiment was performed three times and a representative Southern blot is shown in this figure. DNA derived from Raji cells electroporated with pHEBo-2.2 (lane 3), pHEBo-1.1Δ8353–8994 (lane 5), and pHEBo-1.1Δ8353–8994;9138–9516 (lane 7) was also digested with *Sac*I to separate the fragment derived from the endogenous EBV genome from the test plasmid fragment. The positions of the fragments derived from the EBV genome by digestions with *Eco*RV and *Pst*1 with (lane 2) and without (lane 1) *Sac*1 are indicated on the left and the positions of fragments derived from pHEBo-1, and smaller replicative intermediates are indicated on the right. The arrows on the right indicate the positions at which fragments derived from pHEBo-2.2 and pHEBo-1.1Δ8353–8994 (top arrow), pHEBo-1.1Δ8353–8994;9138–9516 (middle arrow), and pHEBo-1.1 and pHEBo-1.1Δ9138–9516 (bottom arrow) migrated.

also predicted to be highly destabilized in pHEBo-1.1/UAS1 (Fig. 7, panel A) and it replicated as efficiently as pHEBo-1.1 (Fig. 7, panel B).

The ability of a sequence, in which negative superhelicity is predicted to destabilize the DNA by only 2 kcal/mol in several locations (sub4), to substitute functionally for the SIDD region to the left of DS is not surprising when one considers the fact that even relatively small amounts of DNA destabilization can strongly affect the opening process in cases where this process is mediated by a reversible reaction with another molecule. If negative superhelicity destabilizes a region by only 2 kcal/mol (so $G(x) = 8$ kcal/mol), this can drive the equilibrium of the opening reaction more than 25-fold toward the open state, other effects remaining constant. If this opening is the rate-limiting step in a biochemical process, then even small amounts of destabilization can have major effects on the rate of that process. In this regard, it is possible that the modestly destabilized region between EBV nt 8020 and 8353 compensated for the absence of the destabilized region centered on EBV nt 8660 and contributed to the inefficient replication of pHEBo-1.1Δ8353–8994, pHEBo-1.1*sub*1, and pHEBo-1.1*sub*2.

The helix destabilization profiles for *oriP* (Fig. 2) do not predict highly destabilized or denatured sequence elements between EBV nt 9138 and 9516 nor are SIDD structures predicted in this portion of *oriP* when EBV nt 8353–8994 are deleted from pHEBo-1.1 (data not shown). Therefore, it seems unlikely that the dramatic effect of deleting nt 9138–9516 from pHEBo-1.1Δ8353–8994 upon replication efficiency (Table 1) is the result of deleting another helically unstable region. Instead, these results are reminiscent of the multiple functional elements present within *S. cerevisiae* chromosomal replication origins (Marahrens and Stillman, 1992) and the origin of DNA replication of SV40 (Parsons et al., 1990), and suggest that functionally distinct elements located on either side of the EBNA-1/TRF2 binding sites within the replicator contribute to the initiation of DNA replication from within *oriP*.

The ability of four DNA fragments from the EBV genome of similar size but unrelated sequence to increase the replication efficiencies of pHEBo-1.1Δ8353–8994 and pHEBo-1.1Δ8353–8994;9138–9516, albeit to different extents, suggested that the distance between the replicator and an element to the left of the deleted sequence influences replication efficiency. Alternatively, disruption of an *Eco*RV site to the left of the EBNA-1/TRF2 binding sites in the deletion derivatives of pHEBo-1.1 and its restoration in all four substituted plasmids could have been responsible for the increase in replication efficiency of all the pHEBo-1.1*sub*1–4 plasmids. These nucleotides are within a sequence (5'-

Table 1
Replication efficiencies of deletion derivatives of pHEBo-1.1 in Raji cells

Experiment	Test plasmid	Replication efficiencies[a]
1	pHEBo-2.2	<1[b]
	pHEBo-1.1	100[c]
	pHEBo-1.1Δ8353–8994	28 ± 1.6
	pHEBo-1.1Δ9138–9516	50 ± 0.9
	pHEBo-1.1Δ8353–8994;9138–9516	5.6 ± 4.2
2	pHEBo-2.2	1.4 ± 0.45
	pHEBo-1.1	100[d]
	pHEBo-1.1Δ8353–8994	36 ± 8.1
	pHEBo-1.1Δ8353–8991	33 ± 5.0
	pHEBo-1.1Δ8353–8994;9138–9516	6.1 ± 0.57
	pHEBo-1.1Δ8353–8991;9138–9516	6.5 ± 1.5

[a] Replication efficiencies are the percentage of replicated test plasmid DNA in comparison to replicated reference plasmid (pHEBo-1), normalized to pHEBo-1.1 (=100%), per cell generation. The values are the mean ± standard deviation and were derived from three independent determinations.
[b] The replication efficiency of pHEBo-2.2 is reported as <1% as the efficiency was 0.15% in one sample but replicated pHEBo-2.2 DNA was not detected in the other two determinations.
[c] Replication efficiency over three cell generations relative to pHEBo-1 was 125 ± 10%.
[d] Replication efficiency over three cell generations relative to pHEBo-1 was 88 ± 11%.

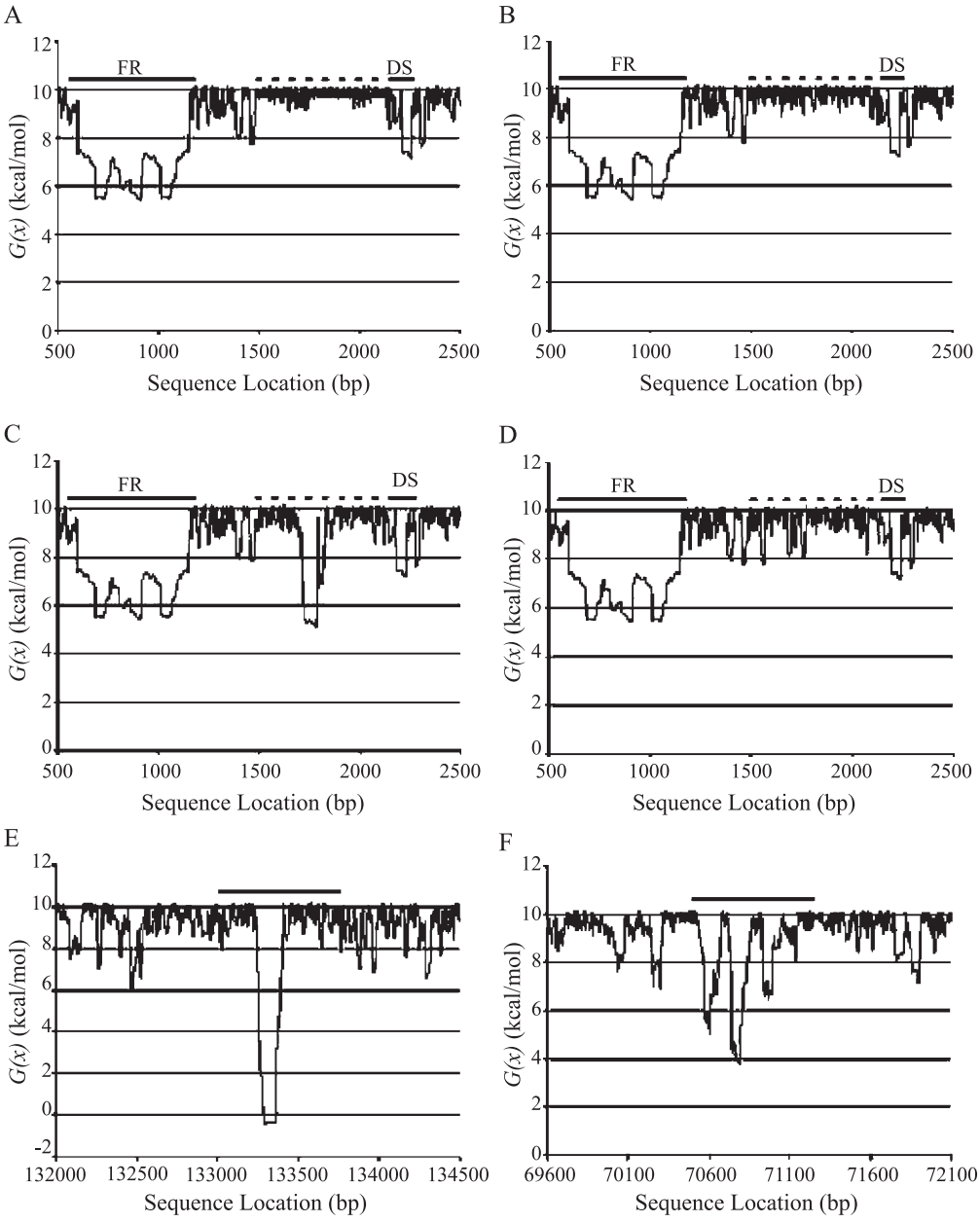

Fig. 5. Helix destabilization profiles for pHEBo-1.1 derivatives containing foreign DNA substituted for the SIDD element within *oriP*. The destabilization profiles show the incremental free energy $G(x)$ required to denature the base pair at position x for *oriP* within pHEBo-1.1 derivatives containing substitutions of helically stable (pHEBo-1.1*sub*1 [panel A] and pHEBo-1.1*sub*2 [panel B]) or helically unstable (pHEBo-1.1*sub*3 [panel C] and pHEBo-1.1*sub*4 [panel D]) DNA. The positions of FR and DS are indicated by bars over the top of each profile. The approximately 650-bp substitutions are indicated by the dashed lines at the top of each profile. Helix destabilization profiles for EBV nt 133 052–133 692 (sub3) and 70 546–71 196 (sub4) in the context of the EBV genome are shown in panels E and F, respectively. The solid bars in panels E and F indicate the DNA fragments used to replace the SIDD element between FR and DS.

GATAT-3') that is present at a similar position within *oriP* of rhesus lymphocryptovirus, a highly related gamma-1 herpesvirus (Rivailler et al., 2002). However, restoration of EBV nt 8992–8994 did not improve the replication efficiency of either pHEBo-1.1 derivative lacking nt 8353–8991 (Table 1), suggesting that the spacing between the EBNA-1/TRF2 binding sites and FR or an unidentified element between the right boundary of FR (nt 8029) and nt 8353 is important for *oriP* function.

Taken together, these results support a role for a region of predicted helically unstable DNA between FR and the replicator of *oriP* in *oriP* function. The DNA sequence encompassing this predicted SIDD structure shares several properties with replication origin DUEs. Both are characterized by helical instability and may be functionally replaced by unrelated sequences that also exhibit helical instability (Kowalski and Eddy, 1989; Umek and Kowalski, 1990). Some DUEs, such as the DUEs of *S. cerevisiae*

Table 2
Replication efficiencies of derivatives of pHEBo-1.1 with unrelated DNA fragments substituted for EBV nt 8534–8994 in Raji cells

Test plasmid	Replication efficiencies[a]
pHEBo-2.2	0.41 ± 0.05
pHEBo-1.1	100[b]
pHEBo-1.1*sub*1	72 ± 3.1
pHEBo-1.1*sub*2	72 ± 5.0
pHEBo-1.1*sub*3	122 ± 7.1
pHEBo-1.1*sub*4	114 ± 6.5
pHEBo-1.1Δ9138–9516;*sub*1	30 ± 2.1
pHEBo-1.1Δ9138–9516;*sub*2	36 ± 6.8
pHEBo-1.1Δ9138–9516;*sub*3	93 ± 7.0
pHEBo-1.1Δ9138–9516;*sub*4	78 ± 5.2

[a] Replication efficiencies are the percentage of replicated test plasmid DNA in comparison to replicated reference plasmid (pHEBo-1), normalized to pHEBo-1.1 (= 100%), per cell generation. The values are the mean ± standard deviation and were derived from three independent determinations.
[b] Replication efficiency over three cell generations relative to pHEBo-1 was 89 ± 11%.

chromosomal replication origins and *oriC* of *E. coli* are hypersensitive to single-strand-specific nucleases in the absence of binding by the origin recognition protein (Kowalski and Eddy, 1989; Natale et al., 1993), but the unwinding of the DUE of the SV40 origin of DNA replication, called the early palindrome, requires the presence of the origin binding protein (Borowiec and Hurwitz, 1988; Parsons et al., 1990). The sequence around EBV bp position 8660 is not predicted to be unwound (Fig. 2) and is not intrinsically sensitive to single-strand-specific nucleases (Orlowski and Miller, 1991; Williams and Kowalski, 1993). Furthermore, we have been unable to identify in vitro conditions in which the binding of EBNA-1 to *oriP* induces unwinding of the DNA around EBV bp position 8700. If this sequence serves as a DUE, it is possible that cellular DNA binding proteins are required for its unwinding. Alternatively, this region of *oriP* may be a component of the replicator that facilitates duplex unwinding at another location. Previous studies of the activation of transcription of the *ilv*P_G promoter of *E. coli* by integration host factor (IHF) have shown that the binding of IHF within a SIDD structure located upstream of the promoter promotes open complex formation through the transfer of superhelical energy to the promoter (Sheridan et al., 1998, 1999). If the SIDD structure coincides with the physical origin of DNA replication within *oriP*, it may be concluded from the results

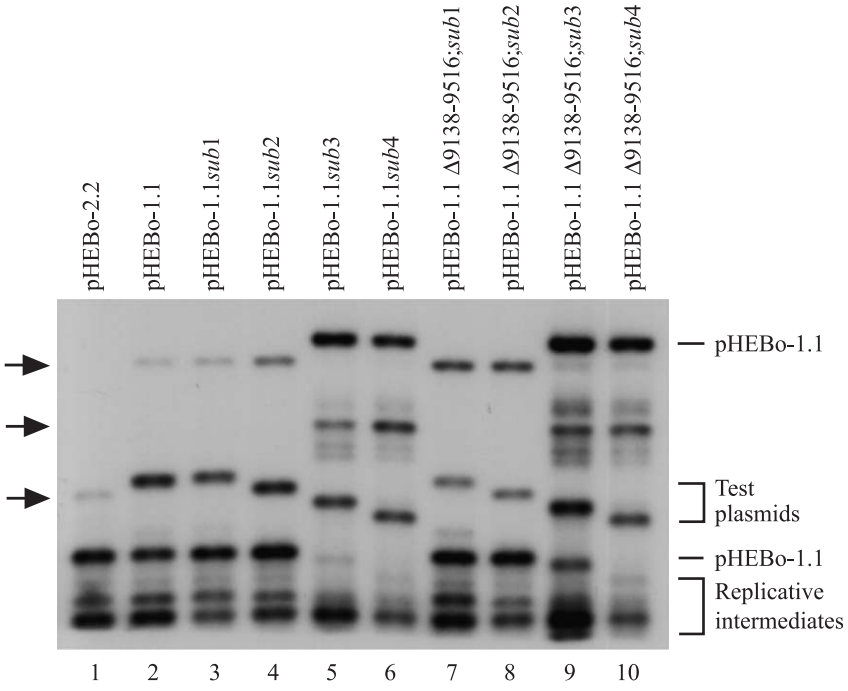

Fig. 6. DNA fragments characterized by high helical instability substitute functionally for EBV nt 8353–8994 within *oriP*. The ability of four fragments of EBV DNA characterized by low (sub1 and sub2) or high (sub3 and sub4) helical instability to substitute functionally for EBV nucleotides 8353–8994 within pHEBo-1.1Δ8353–8994 and pHEBo-1.1Δ8353–8994;9138–9516 was determined as described in the legend for Fig. 3 and Materials and methods, and a representative Southern blot showing the results of one of three determinations is presented in this figure. The test plasmids co-electroporated with pHEBo-1 are indicated above each lane. The three different fragments produced by digestion of EBV DNA with one of three combinations of restriction enzymes used in this experiment to separate the test plasmid from pHEBo-1 and EBV DNA are indicated by arrows on the left side of the figure. The top arrow indicates the position of the EBV genome fragment in lanes 2, 3, 4, 7, and 8. The middle arrow shows the position of the EBV genome fragment in lanes 5, 6, 9, and 10. The bottom arrow indicates the position of the EBV genome fragment in lane 1. The positions of the fragments derived from pHEBo-1 and the test plasmids are indicated on the right side of the figure. The different mobilities of the test plasmid-derived fragments are due to differences in the positions of restriction enzyme sites and not the size of the substituted DNA. The DNA fragments migrating between the fragment derived from pHEBo-1 and the fragments derived from pHEBo-1.1*sub*3 (lane 5), pHEBo-1.1*sub*4 (lane 6), pHEBo-1.1Δ9138–9516;*sub*3 (lane 9), and pHEBo-1.1Δ9138–9516;*sub*4 (lane 10) are pHEBo-1-replicative intermediates.

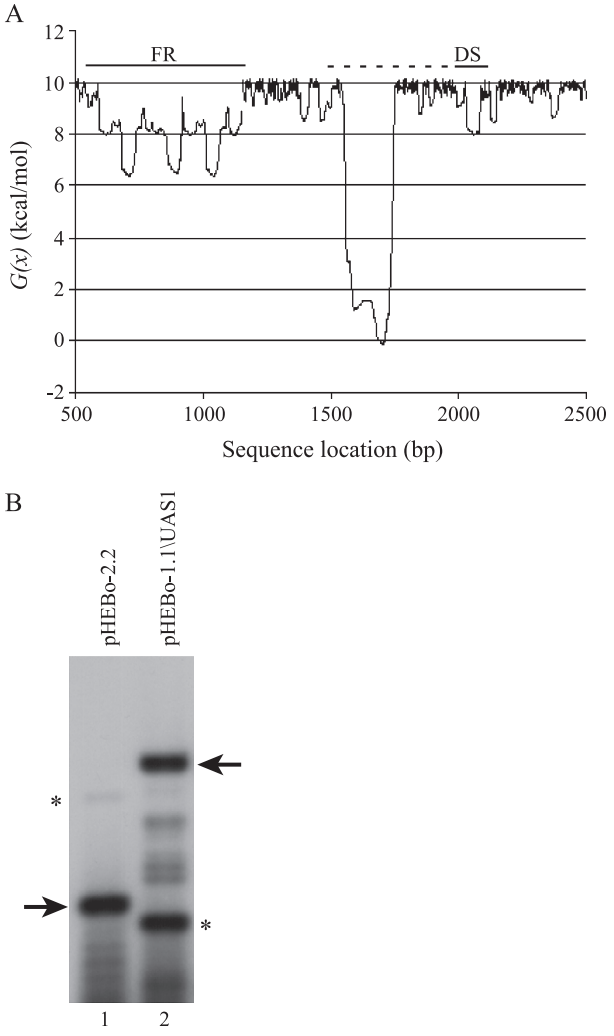

Fig. 7. The *E. coli ilv*P_G UAS1 rescues the replication defect of pHEBo-1.1Δ8353–8994. A helix destabilization profile showing the instability of the *ilv*P_G UAS1 in pHEBo-1.1/UAS1 is shown in panel A. The solid bars indicate the locations of FR and DS, and the dashed line indicates the position of the DNA fragment harboring the *ilv*P_G UAS1. Panel B shows the result of a representative short-term replication assay performed with pHEBo-2.2 and pHEBo-1.1 (lane 1) and pHEBo-1.1/UAS1 and pHEBo-1.1 (lane 2). The arrows show the bands derived from the reference plasmid pHEBo-1.1 and the asterisks indicate the bands derived from the test plasmids. The faint bands between the reference and test plasmid bands in lane 2 represent replicative intermediates of pHEBo-1.1.

presented here that other regions within *oriP* may be used inefficiently in its absence.

Materials and methods

Plasmids

The parental plasmids used in this study, pHEBo-1 and pHEBo-1.1, both contain all of *oriP* and differ solely in the absence of 342 bp in the portion of the plasmids derived from pBR322 from pHEBo-1.1 that allows the plasmids to be distinguished in short-term replication assays (Hearing et al., 1992; Sugden et al., 1985). pHEBo-1.1Δ9138–9516 and a replication-defective deletion derivative that lacks EBV nt 8995–9137, pHEBo-2.2, have been described previously (Koons et al., 2001). pHEBo-1.1Δ8353–8994 and pHEBo-1.1Δ8353–8994;9138–9516 were derived by deleting 642 bp between the unique *Msc*1 and *Eco*RV sites of pHEBo-1.1 and pHEBo-1.1Δ9138–9516, respectively. Regions of EBV DNA substituted for EBV nt 8353–8994 in pHEBo-1.1 and pHEBo-1.1Δ9138–9516 were obtained by PCR amplification using plasmids harboring restriction enzyme fragments of EBV DNA (B95-8 isolate) as template (Dambaugh et al., 1980). The EBV nucleotide coordinates for these regions are 12,051–12,700 (sub1), 3996–4644 (sub2), 133,052–133,692 (sub3), and 70,546–71,196 (sub4). Together with the addition of nucleotides at the ends of the PCR fragments to facilitate cloning, the inserts in the subplasmids were 672 bp (sub1), 650 bp (sub2), 640 bp (sub3), and 654 bp (sub4). EBV nucleotides 8991–8993 were restored to pHEBo-1.1Δ8353–8994 and pHEBo-1.1Δ8353–8994;9138–9516 by ligating an oligonucleotide linker containing *Eco*RV ends with the large fragment produced by digestion of pHEBo-1.1 and pHEBo-1.1Δ9138–9516 plasmid DNA with *Msc*I and *Eco*RV. The ends of an *Eco*RI–*Hin*dIII fragment from pDHΔWT, containing the *E. coli ilv*P_G UAS1, were repaired with Klenow DNA polymerase and the fragment was ligated with the large *Eco*RV–*Msc*I fragment of pHEBo-1.1 to create pHEBo-1.1/UAS1.

Short-term replication assays

The replication efficiencies of pHEBo-1.1 derivatives (with the exception of pHEBo-1.1/UAS1) were determined by co-electroporating Raji cells with a reference plasmid that replicates once per cell cycle (pHEBo-1) (Yates and Guan, 1991) and the test plasmid. Electroporated cells were maintained in a constantly dividing state for 72 h at which time low molecular weight DNA was isolated. Samples were digested with *Dpn*I and a combination of other restriction enzymes that produced fragments from the endogenous EBV genome, pHEBo-1, and the test plasmid that could be readily distinguished upon agarose gel electrophoresis (*Eco*RV and *Pst*I for pHEBo-1.1, pHEBo-1.1Δ9138–9516, pHEBo-1.1*sub*1, pHEBo-1.1*sub*2, pHEBo-1.1Δ9138–9516;*sub*1, pHEBo-1.1Δ9138–9516;*sub*2, pHEBo-1.1Δ8353–8991, pHEBo-1.1Δ8353–8991;9138–9516; *Eco*RV, *Pst*I, and *Sac*I for pHEBo-2.2, pHEBo-1.1Δ8353–8994, pHEBo-1.1Δ8353–8994;9138–9516; *Pst*I and *Sac*I for pHEBo-1.1*sub*3, pHEBo-1.1*sub*4, pHEBo-1.1Δ9138–9516;*sub*3, pHEBo-1.1Δ9138–9516;*sub*4). Digests were analyzed by Southern blotting using a *Bam*HI–*Msc*I fragment bearing *oriP* FR from pHEBo-1 and the amount of probe that hybridized to the plasmid-derived fragments was quantitated with a Molecular Dynamics Storm 860 phosphorimager and ImageQuant software. The relative amount of replicated test and reference plasmid DNA in each sample was corrected for

the ratio of the two plasmids in the sample used for electroporation and the replication efficiencies of the test plasmids were calculated. Statistical analysis of the replication efficiencies was performed by one-way analysis of variance and by using Tukey's "honestly significant difference" test to make pair-wise comparisons. A detailed description of this assay may be found in Koons et al. (2001).

The replication efficiency of pHEBo-1.1/UAS1 was determined by co-transfecting the EBNA-1-positive cell line 293-EBNA (Invitrogen) with 3 μg each pHEBo-1.1/UAS1 and pHEBo-1.1 using the calcium phosphate co-precipitation method (Graham et al., 1977). A parallel culture was co-transfected with 3 μg each pHEBo-2.2 and pHEBo-1.1. The medium containing the calcium phosphate-DNA co-precipitates was replaced with fresh medium after 16 h at 37 °C and low molecular weight DNA was isolated from the cells 72 h following transfection (Hirt, 1967). DNA isolated from 293-EBNA cells co-transfected with pHEBo-2.2 and pHEBo-1.1 was digested with *Dpn*I, *Eco*RV, and *Pst*I while DNA isolated from cells co-transfected with pHEBo-1.1/UAS1 and pHEBo-1.1 was digested with *Dpn*I and *Pst*I. The digested samples were analyzed by Southern blotting using a *Bam*HI–*Msc*I fragment bearing *oriP* FR from pHEBo-1 as the probe as described above.

Analysis of sequences for predicted stress-induced duplex destabilization

Theoretical analysis of the unwinding propensity of the experimental plasmid at various superhelix densities was performed using the technique previously developed by Benham (1992, 1993). This method calculates the statistical mechanical equilibrium distribution of a population of identical, superhelical DNA molecules among all available states of denaturation. It then evaluates the equilibrium probability $p(x)$ of denaturation at single base pair resolution. It also calculates the destabilization energy $G(x)$, the incremental free energy required to assure that the base pair at position x is denatured. Thus, high values of $G(x)$ occur at positions where the duplex is relatively stable, and low values at easily stress-destabilized sites. Positions where $G(x)$ is near zero are denatured with high probability at equilibrium under the assumed level of superhelicity. The calculation of $G(x)$ enables one to find fractionally destabilized sites—locations that have a low equilibrium probability of denaturation, but where other processes can drive duplex opening with a relatively small incremental input of energy.

All the free energy and conformational parameters used in these calculations have been experimentally measured, usually in multiple ways and under a variety of environmental conditions. So there are no free (i.e., tunable) parameters in these analyses. Yet their results have been shown to be in quantitative agreement with experiment in all cases where experiments have been performed. They accurately predict both the locations and the extents of destabilization experienced by a DNA molecule of known base sequence, on which a specific level of superhelicity has been imposed.

DNA denaturation behaves differently when it is driven by superhelicity within topological domains than it does when driven by temperature in unconstrained molecules. In the latter case, only near neighbor effects are involved. In the former, the superhelical constraint couples together the behaviors of all base pairs within the domain. This coupling occurs because denaturation of any base pair alters its twist, which changes the partitioning of the superhelicity throughout the domain. In this way, every base pair is affected by the denaturation of any other base pair. This makes the transition behavior of a domain potentially complex and interactive, with the opening of some regions coupled to the reversion back to B-form of others. For this reason, thermodynamic stability is not an adequate predictor of stress-induced destabilization (Benham, 1996).

The calculations reported here were performed using the energy parameters appropriate for the nuclease digestion procedure of Kowalski et al. (1988) at a variety of superhelix densities as described.

Acknowledgments

We thank G. Wesley Hatfield for pDHΔWT, Sally Madden for assistance in preparation of figures, and Patrick Hearing for critical review of the manuscript. This work was supported by grants from the National Cancer Institute (CA75992 to J.H.), the NHGRI (HG01973 to C.J.B), and the National Science Foundation (DBI-99-04549 to C.J.B.).

References

Adams, A., 1987. Replication of latent Epstein–Barr virus genomes in Raji cells. J. Virol. 61, 1743–1746.

Bashaw, J.M., Yates, J.L., 2001. Replication from *oriP* of Epstein–Barr virus requires exact spacing of two bound dimers of EBNA1 which bend DNA. J. Virol. 75, 10603–10611.

Benham, C.J., 1992. Energetics of the strand separation transition in superhelical DNA. J. Mol. Biol. 225, 835–847.

Benham, C.J., 1993. Sites of predicted stress-induced DNA duplex destabilization occur preferentially at regulatory loci. Proc. Natl. Acad. Sci. U.S.A. 90, 2999–3003.

Benham, C.J., 1996. Duplex destabilization in superhelical DNA is predicted to occur at specific transcriptional regulatory regions. J. Mol. Biol. 255, 425–434.

Borowiec, J.A., Hurwitz, J., 1988. Localized melting and structural changes in the SV40 origin of replication induced by T-antigen. EMBO J. 7, 3149–3158.

Chaudhuri, B., Xu, H., Todorov, I., Dutta, A., Yates, J.L., 2001. Human DNA replication initiation factors, ORC and MCM, associate with *oriP* of Epstein–Barr virus. Proc. Natl. Acad. Sci. U.S.A. 98, 10085–10089.

Dambaugh, T., Beisel, C., Hummel, M., King, W., Fennewald, S., Cheung, A., Heller, M., Raab-Traub, N., Kieff, E., 1980. Epstein–Barr virus (B95–8) DNA VII: molecular cloning and detained mapping. Proc. Natl. Acad. Sci. U.S.A. 77, 2999–3003.

Deng, Z., Lesina, L., Chen, C.-J., Shtivelband, S., So, W., Lieberman, P.M., 2002. Telomeric proteins regulate episomal maintenance of Epstein–Barr virus origin of plasmid replication. Mol. Cell 9, 493–503.

Frappier, L., O'Donnell, M., 1992. EBNA1 distorts *oriP*, the Epstein–Barr virus latent replication origin. J. Virol. 66, 1786–1790.

Gahn, T.A., Schildkraut, C.L., 1989. The Epstein–Barr virus origin of plasmid replication, *oriP*, contains both the initiation and termination sites of DNA replication. Cell 58, 527–535.

Graham, F.L., Smiley, J., Russell, W.C., Nairn, R., 1977. Characterization of a human cell line transformed by DNA from human adenovirus type 5. J. Gen. Virol. 36, 59–72.

Harrison, S., Fisenne, K., Hearing, J., 1994. Sequence requirements of the Epstein–Barr virus latent origin of DNA replication. J. Virol. 68, 1913–1925.

Hearing, J., Mülhaupt, Y., Harper, S., 1992. Interaction of Epstein–Barr virus nuclear antigen 1 with the viral latent origin of replication. J. Virol. 66, 694–705.

Hirt, B., 1967. Selective extraction of polyoma DNA from infected mouse cell cultures. J. Mol. Biol. 26, 365–369.

Hsieh, D.J., Camiolo, S.M., Yates, J.L., 1993. Constitutive binding of EBNA1 protein to the Epstein–Barr virus replication origin, *oriP*, with distortion of DNA structure during latent infection. EMBO J. 12, 4933–4944.

Koons, M.D., Van Scoy, S., Hearing, J., 2001. The replicator of the Epstein–Barr virus latent cycle origin of DNA replication, *oriP*, is composed of multiple functional elements. J. Virol. 75, 10582–10592.

Kowalski, D., Eddy, M.J., 1989. The DNA unwinding element: a novel, cis-acting component that facilitates opening of the *Escherichia coli* replication origin. EMBO J. 8, 4335–4344.

Kowalski, D., Natale, D.A., Eddy, M.J., 1988. Stable DNA unwinding, not "breathing", accounts for single-strand-specific nuclease hypersensitivity of specific A + T-rich sequences. Proc. Natl. Acad. Sci. U.S.A. 85, 9464–9468.

Lin, S., Kowalski, D., 1994. DNA helical instability facilitates initiation at the SV40 replication origin. J. Mol. Biol. 235, 496–507.

Lin, S., Kowalski, D., 1997. Functional equivalency and diversity of cis-acting elements among yeast replication origins. Mol. Cell. Biol. 17, 5473–5484.

Little, R.D., Schildkraut, C.L., 1995. Initiation of latent DNA replication in the Epstein–Barr virus genome can occur at sites other than the genetically defined origin. Mol. Cell. Biol. 15, 2893–2903.

Marahrens, Y., Stillman, B., 1992. A yeast chromosomal origin of DNA replication defined by multiple functional elements. Science 255, 817–823.

Mecsas, J., Sugden, B., 1987. Replication of plasmids derived from bovine papilloma virus type 1 and Epstein–Barr virus in cells in culture. Annu. Rev. Cell Biol. 3, 87–108.

Natale, D.A., Schubert, A.E., Kowalski, D., 1992. DNA helical instability accounts for mutational defects in a yeast replication origin. Proc. Natl. Acad. Sci. U.S.A. 89, 2654–2658.

Natale, D.A., Umek, R.M., Kowalski, D., 1993. Ease of DNA unwinding is a conserved property of yeast replication origins. Nucleic Acids Res. 21, 555–560.

Norio, P., Schildkraut, C.L., 2001. Visualization of DNA replication on individual Epstein–Barr virus episomes. Science 294, 2361–2364.

Norio, P., Schildkraut, C.L., Yates, J.L., 2000. Initiation of DNA replication within oriP is dispensable for stable replication of the latent Epstein–Barr virus chromosome after infection of established cell lines. J. Virol. 74, 8563–8574.

Orlowski, R., Miller, G., 1991. Single-stranded structures are present within plasmids containing the Epstein–Barr virus latent origin of replication. J. Virol. 65, 677–686.

Parsons, R., Anderson, M.E., Tegtmeyer, P., 1990. Three domains in the simian virus 40 core antigen orchestrate the binding, melting, and DNA helicase activities of T antigen. J. Virol. 64, 509–518.

Reisman, D., Yates, J., Sugden, B., 1985. A putative origin of replication of plasmids derived from Epstein–Barr virus is composed of two cis-acting components. Mol. Cell. Biol. 5, 1822–1832.

Rivailler, P., Jiang, H., Cho, Y.-G., Quink, C., Wang, F., 2002. Complete nucleotide sequence of the rhesus lymphocryptovirus: genetic validation for an Epstein–Barr virus animal model. J. Virol. 76, 421–426.

Schepers, A., Ritzi, M., Bousset, K., Kremmer, E., Yates, J.L., Harwood, J., Diffley, J.X.F., Hammerschmidt, W., 2001. Human origin recognition complex binds to the region of the latent origin of DNA replication of Epstein–Barr virus. EMBO J. 20, 4588–4602.

Sheridan, S.D., Benham, C.J., Hatfield, G.W., 1998. Activation of gene expression by a novel DNA structural transmission mechanism that requires supercoiling-induced DNA duplex destabilization in an upstream activating sequence. J. Biol. Chem. 273, 21298–21308.

Sheridan, S.D., Benham, C.J., Hatfield, G.W., 1999. Inhibition of DNA supercoiling-dependent transcriptional activation by a distant B-DNA to Z-DNA transition. J. Biol. Chem. 274, 8169–8174.

Shirakata, M., Hirai, K., 1998. Identification of minimal oriP of Epstein–Barr virus required for DNA replication. J. Biochem. 123, 175–181.

Shirakata, M., Imadome, K.I., Hirai, K., 1999. Requirement of replication licensing for the dyad symmetry element-dependent replication of the Epstein–Barr virus *oriP* minichromosome. Virology 263, 42–54.

Sugden, B., Marsh, K., Yates, J., 1985. A vector that replicates as a plasmid and can be efficiently selected in B-lymphoblasts transformed by Epstein–Barr virus. Mol. Cell. Biol. 5, 410–413.

Umek, R.M., Kowalski, D., 1988. The ease of DNA unwinding as a determinant of initiation at yeast replication origins. Cell 52, 559–567.

Umek, R.M., Kowalski, D., 1990. Thermal energy suppresses mutational defects in DNA unwinding at a yeast replication origin. Proc. Natl. Acad. Sci. U.S.A. 87, 2486–2490.

Williams, D.L., Kowalski, D., 1993. Easily unwound DNA sequences and hairpin structures in the Epstein–Barr virus origin of plasmid replication. J. Virol. 67, 2707–2715.

Yates, J.L., 1996. Epstein–Barr virus DNA replication. In: DePamphilis, M.L. (Ed.), DNA Replication in Eukaryotic Cells. Cold Spring Harbor Laboratory Press, Cold Spring Harbor, NY, pp. 751–773.

Yates, J.L., Camiolo, S.M., Bashaw, J.M., 2000. The minimal replicator of Epstein–Barr virus *oriP*. J. Virol. 74, 4512–4522.

Yates, J.L., Guan, N., 1991. Epstein–Barr virus-derived plasmids replicate only once per cell cycle and are not amplified after entry into cells. J. Virol. 65, 483–488.

Yates, J., Warren, N., Reisman, D., Sugden, B., 1984. A cis-acting element from the Epstein–Barr viral genome that permits stable replication of recombinant plasmids in latently infected cells. Proc. Natl. Acad. Sci. U.S.A. 81, 3806–3810.

Yates, J.L., Warren, N., Sugden, B., 1985. Stable replication of plasmids derived from Epstein–Barr virus in various mammalian cells. Nature 313, 812–815.